Systematic comparison of jet energy-loss schemes in a realistic hydrodynamic medium

Steffen A. Bass,[1] Charles Gale,[2] Abhijit Majumder,[1] Chiho Nonaka,[3] Guang-You Qin,[2] Thorsten Renk,[4,5] and Jörg Ruppert[2]

[1]*Department of Physics, Duke University, Durham, North Carolina 27708, USA*

[2]*Department of Physics, McGill University, H3A 2T8, Montreal, Quebec, Canada*

[3]*Department of Physics, Nagoya University, Nagoya 464-8602, Japan*

[4]*Department of Physics, University of Jyväskylä, P. O. Box 35, FI-40014, Finland*

[5]*Helsinki Institute of Physics, University of Helsinki, P. O. Box 64, FI-00014, Finland*

(Received 13 August 2008; published 5 February 2009)

We perform a systematic comparison of three different jet energy-loss approaches. These include the Armesto-Salgado-Wiedemann scheme based on the approach of Baier-Dokshitzer-Mueller-Peigne-Schiff and Zakharov (BDMPS-Z/ASW), the higher twist (HT) approach and a scheme based on the Arnold-Moore-Yaffe (AMY) approach. In this comparison, an identical medium evolution will be utilized for all three approaches: this entails not only the use of the same realistic three-dimensional relativistic fluid dynamics (RFD) simulation, but also the use of identical initial parton-distribution functions and final fragmentation functions. We are, thus, in a unique position to not only isolate fundamental differences between the various approaches but also make rigorous calculations for different experimental measurements using state of the art components. All three approaches are reduced to versions containing only one free tunable parameter, this is then related to the well-known transport parameter $\hat{q}$. We find that the parameters of all three calculations can be adjusted to provide a good description of inclusive data on R_{AA} vs transverse momentum. However, we do observe slight differences in their predictions for the centrality and azimuthal angular dependence of R_{AA} vs p_T. We also note that the values of the transport coefficient $\hat{q}$ in the three approaches to describe the data differ significantly.

DOI: 10.1103/PhysRevC.79.024901 PACS number(s): 25.75.Nq, 25.75.Bh, 12.38.Mh, 12.38.Bx

I. INTRODUCTION

The first seven years of operations at the BNL Relativistic Heavy Ion Collider (RHIC), which entailed performing collisions of gold nuclei at $\sqrt{s}_{NN} = 130$ and $\sqrt{s}_{NN} = 200$ GeV, have yielded a vast amount of interesting and sometimes surprising results [1–4]. Many of these have not yet been fully evaluated or understood by theory. There exists mounting evidence that RHIC has created a hot and dense state of deconfined QCD matter with properties similar to those of an ideal fluid [5]; this state of matter has been termed the *strongly interacting quark-gluon plasma* (sQGP).

RHIC has generated a wealth of experimental data on high-momentum hadron emission, including, but not limited to, the nuclear modification factor R_{AA}, its modification as a function of the reaction plane (a measure of the azimuthal anisotropy of the cross section), and a whole array of high-p_T hadron-hadron correlations. In these observables, one compares the ratio of certain yields in a heavy-ion collision to those in a p-p collision, either scaled up by the number of expected binary collisions, e.g., for the single hadron suppression factor R_{AA}, or directly, as in the case of triggered distributions of associated hadrons, e.g., the I_{AA} [6–8]. Experimental data for most of these observables exist as functions of rapidity and centrality for a wide range of p_T of the produced particle or particles.

The emission of hadrons with large transverse momentum is observed to be strongly suppressed in central collisions of heavy nuclei [9,10]. The origin of this phenomenon, commonly referred to as *jet-quenching*, can be understood in the following way: during the early pre-equilibrium stage of the relativistic heavy-ion collision, scattering of partons which leads to the formation of deconfined quark-gluon matter often engenders large momentum transfers which leads to the formation of two back-to-back hard partons. These traverse the dense medium, losing energy, and finally fragment into hadrons, which are observed by the experiments. Within the framework of perturbative QCD, the process with the largest energy loss of a fast parton is gluon radiation induced by collisions with the quasithermal medium [11–19].

Computations of jet modification have acquired a certain sophistication in the incorporation of the partonic processes involved. However, the role of the medium has often been relegated to the furnishing of an overall density and its variation with time [20–23]. Notable departures from these simple treatments include attempts to incorporate radial expansion, both schematically [24,25] as well as within a fireball evolution model [26]. The first attempt to incorporate energy loss in a three-dimensional (3D) relativistic fluid dynamical (RFD) simulation was carried out by Hirano and Nara [27]. In that effort, while a full 3D RFD simulation was used, the energy loss of hard jets was carried out rather schematically. This approach was also extended to the case of two particle correlations in Ref. [28]. In a later effort, the authors also incorporated a simplified version of the Gyulassy-Levai-Vitev (GLV) energy-loss formalism at leading order in opacity [29].

Besides the simplified version of the GLV formalism used, the authors attempted to apply the results to the region of $p_T \leqslant 6$ GeV, which is the region where data were available at the time. In spite of the success of Ref. [29] in explaining the suppression of single inclusive pions, such a formalism cannot address the flavor dependence of the elliptic flow in this region of p_T. It has since been established that jet fragmentation in vacuum is not the primary mechanism of hadronization in the

range of $p_T < 6$ GeV, and there is a sizable component which arises from recombination. Current rigorous implementations of jet modification in dense matter require that the p_T of the detected hadron be above 6 GeV. This requirement allows the final hadronization to be treated using the standard vacuum fragmentation functions, and the ability of a given energy-loss formalism to compare with experimental data is then dependent solely on the details of the interaction of the parton with the medium in that formalism. This allows a comparison to be made between formalisms in which all other components of the calculation, such as the initial parton distribution, the final fragmentation function, and the space-time profile of the medium, are identical. This article presents the first attempt to perform such a comparison between the remaining three formalisms: the Armesto-Salgado-Wiedemann scheme based on the approach of Baier-Dokshitzer-Mueller-Peigne-Schiff and Zakharov (BDMPS-Z/ASW), the higher twist (HT) approach and a scheme based on the Arnold-Moore-Yaffe (AMY) approach.

Besides just a comparison between formalisms, this paper will also apply the different formalisms in comparison data. A realistic comparison with data requires a sophisticated model of the medium. The availability of a 3D hydrodynamic evolution code [30] allows a much more detailed study of jet interactions in a longitudinally and transversely expanding medium. The variation of the gluon density in such a medium is quite different from that in a simple Bjorken expansion. This allows a step-by-step approach to the study of jet-medium interactions. Over the past year, we have already utilized our evolution model to provide the time evolution of the medium produced at RHIC for jet energy-loss calculations performed in the BDMPS-Z/ASW [31], HT [32], and AMY [33] approaches. In each of the three projects, the inclusive as well as the azimuthally differential nuclear suppression factor R_{AA} of pions was studied as a function of their transverse momentum p_T. In addition, the influence of collective flow, variations in rapidity, and energy loss in the hadronic phase were addressed for the selected approaches.

In this manuscript, we shall perform a systematic comparison of jet energy-loss calculations in the BDMPS-Z/ASW, HT, and AMY approaches. Since we use the same medium evolution in all three approaches, we are in a position to isolate differences among the three calculations solely due to their energy-loss schemes. This will allow us to answer the question of whether the observed differences between the different schemes (when compared with data) are due to differing treatment of the medium evolution and its coupling to the energy-loss calculation or whether they are rooted in more fundamental issues related to the energy-loss schemes themselves, e.g., as a result of the approximations and assumptions made when deriving the respective schemes.

In Sec. II, we briefly review the 3D hydrodynamic description of the medium. We then discuss in Sec. III the theoretical setup of different energy-loss schemes and their connection to the 3D dynamical evolving medium. Numerical results are presented in comparison with the available RHIC data in Sec. IV. In Sec. V, we discuss issues related to further comparisons of our calculations with the data on R_{AA} vs the reaction plane, and we present concluding discussions and an outlook for future work in Sec. VI.

II. HYDRODYNAMIC DESCRIPTION OF THE MEDIUM

Relativistic fluid dynamics (RFD) simulations (see, e.g., Refs. [34–36]) is ideally suited for the high-density phase of heavy-ion reactions at RHIC, but break down in the later, dilute stages of the reaction when the mean free paths of the hadrons become large and flavor degrees of freedom are important. The biggest advantage of RFD is that it directly incorporates an equation of state as input and thus is so far the only dynamical model in which a phase transition can explicitly be incorporated. The starting point for a RFD calculation is the relativistic hydrodynamic equation

$$\partial_\mu T^{\mu\nu} = 0, \tag{1}$$

where $T^{\mu\nu}$ is the energy momentum tensor given by

$$T^{\mu\nu} = (\epsilon + p)U^\mu U^\nu - p g^{\mu\nu}. \tag{2}$$

Here ϵ, p, U, and $g^{\mu\nu}$ are energy density, pressure, four-velocity, and metric tensor, respectively. The relativistic hydrodynamic equation [Eq. (1)] is solved numerically using baryon number n_B conservation

$$\partial_\mu (n_B(T, \mu)U^\mu) = 0 \tag{3}$$

as a constraint and closing the resulting set of partial differential equations by specifying an equation of state (EOS): $\epsilon = \epsilon(p)$. In the ideal fluid approximation (i.e., neglecting off-equilibrium effects) and once the initial conditions for the calculation have been fixed, the EOS is the *only* input to the equations of motion and relates directly to properties of the matter under consideration. Ideally, either the initial conditions or the EOS should be determined beforehand by an *ab-initio* calculation (e.g., for the EOS via a lattice-gauge calculation), in which case a fit to the data would allow the determination of the remaining quantity. Our particular RFD implementation utilizes a Lagrangian mesh and light-cone coordinates, i.e., (τ, x, y, η) where $\tau = \sqrt{t^2 - z^2}$ is the proper time and η is the pseudorapidity. This is done to optimize the model for the ultrarelativistic regime of heavy collisions at RHIC.

We assume that hydrodynamic expansion starts at $\tau_0 = 0.6$ fm. Initial energy density and baryon number density are parametrized by

$$\begin{aligned} \epsilon(x, y, \eta) &= \epsilon_{\max} W(x, y; b) H(\eta), \\ n_B(x, y, \eta) &= n_{B\max} W(x, y; b) H(\eta), \end{aligned} \tag{4}$$

where b and $\epsilon_{\max}$ ($n_{B\max}$) are the impact parameter and the maximum value of energy density (baryon number density), respectively. $W(x, y; b)$ is given by a combination of wounded nuclear model and binary collision model [37], and $H(\eta)$ is given by $H(\eta) = \exp[-(|\eta| - \eta_0)^2/2\sigma_\eta^2 \cdot \theta(|\eta| - \eta_0)]$. RFD has been very successful in describing single soft matter properties at RHIC, especially collective flow effects and particle spectra [30,38–40]. All parameters of our hydrodynamic evolution [30] have been fixed by a fit to the soft sector (elliptic flow, pseudorapidity distributions, and low-p_T single-particle spectra), therefore providing us with a fully

determined medium evolution for the hard probes to propagate through.

III. JET ENERGY-LOSS SCHEMES

The majority of current approaches to the energy loss of light partons may be divided into four major schemes often referred to by the names of the original authors:

(i) Higher twist (HT) [41–46]
(ii) Path integral approach to the opacity expansion (BDMPS-Z/ASW) [14,15,17–19,21,47–50]
(iii) Finite temperature field theory approach (AMY) [22,51–53]
(iv) Reaction operator approach to the opacity expansion (GLV) [20,54–57]

All schemes utilize a factorized approach in which the final cross section to produce a hadron h with transverse momentum p_T (rapidity between y and $y + dy$) may be expressed as a convolution of initial nuclear structure functions [$G_a^A(x_a)$,$G_b^B(x_b)$, initial state nuclear effects such as shadowing and Cronin effect are understood to be included] to produce partons with momentum fractions x_a, x_b, a hard partonic cross section to produce a high transverse momentum parton c with a transverse momentum $\hat{p}$, and a medium-modified fragmentation function for the final hadron [$\tilde{D}_c^h(z)$], that is,

$$\frac{d^2\sigma^h}{dyd^2p_T} = \frac{1}{\pi}\int dx_a \int dx_b G_a^A(x_a) G_b^B(x_b) \times \frac{d\sigma_{ab\to cX}}{d\hat{t}} \frac{\tilde{D}_c^h(z)}{z}. \quad (5)$$

In the vicinity of midrapidity, $z = p_T/\hat{p}$ and $\hat{t} = (\hat{p} - x_a P)^2$ (P is the average incoming momentum of a nucleon in nucleus A). The entire effect of energy loss is concentrated in the calculation of the modification to the fragmentation function.

The four models of energy loss are in a sense four schemes to estimate this quantity from perturbative QCD calculations. While the terminology (medium modification) used to describe the change in the fragmentation function seems to indicate that the medium has influenced the actual process of the formation of the final hadrons from the partonic cloud, this is not the case. All computations simply describe the change in the gluon radiation spectrum from a hard parton due to the presence of the medium. The final hadronization of the hard parton is always assumed to occur in the vacuum after the parton, with degraded energy, has escaped from the medium. Note that some of the hard gluons radiated from the hard parton will also encounter similar "modification" in the medium and may endure vacuum hadronization after escaping from the medium. Differences between formalisms also arise in the inclusion of hadrons from the fragmentation of such subleading gluons: whereas approaches that compute the change in the distribution of final partons (such as AMY) or the change in the distribution of final hadrons (such as HT) implicitly include hadrons from subleading gluons, formalisms that compute the energy loss of the leading parton (such as ASW) do not include such subleading corrections.

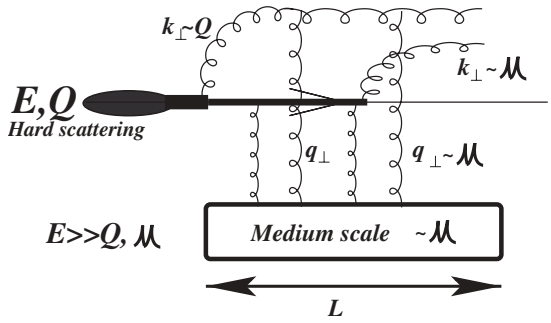

FIG. 1. A schematic picture of the various scales involved in the modification of jets in dense matter.

To better appreciate the approximation schemes, one may introduce a set of scales (see Fig. 1): E or p^+, the forward energy of the jet; Q^2, the virtuality of the initial jet-parton; μ, the momentum scale of the medium; and L, its spatial extent. Most of the differences between the various schemes may be reduced to the different relations between these various scales assumed by each scheme as well as by how each scheme treats or approximates the structure of the medium. In all schemes, the forward energy of the jet far exceeds the medium scale, $E \gg \mu$. The schemes are presented from one extreme of the approximation set (higher twist approach) to the opposite extreme (finite temperature approach), similarities in intermediate steps of the calculation will not be repeated. In the following, we will focus on the first three listed approaches, for which we will present results in Sec. IV (note that a calculation of GLV jet energy loss in a 3D hydrodynamic medium has been presented elsewhere [29]).

A. Higher Twist Formalism

The origin of the HT approximation scheme lies in the calculations of medium-enhanced higher twist corrections to the total cross section in deep inelastic scattering (DIS) off large nuclei [58]. One resums power corrections to the leading twist cross sections, which, though suppressed by powers of the hard scale Q^2, are enhanced by the length of the medium. This technology of identifying and isolating power corrections is used to compute the n-hadron inclusive cross section.

One assumes the hierarchy of scales $E \gg Q \gg \mu$ and applies this to the computation of multiple Feynman diagrams such as the one in Fig. 2; this diagram represents the process

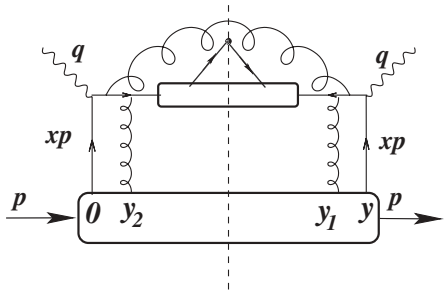

FIG. 2. Typical higher twist contribution used to compute the modification of the fragmentation function in medium.

of a hard virtual quark produced in a hard collision, which radiates a gluon and then scatters off a soft medium gluon with transverse momentum $q_\perp \sim \mu$ prior to exiting the medium and fragmenting into hadrons. At a given order, various other contributions exist that involve scattering of the initial quark off the soft gluon field prior to radiation as well as scattering of the radiated gluon itself. All such contributions are combined coherently to calculate the modification to the fragmentation function directly.

The hierarchy of scales allows one to use the collinear approximation to factorize the fragmentation function and its modification from the hard scattering cross section. Thus, even though such a modified fragmentation function is derived in DIS, it may be generalized to the kinematics of a heavy-ion collision. Diagrams in which the outgoing parton scatters off the medium gluons, such as those in Fig. 2, produce a medium-dependent additive contribution to the vacuum fragmentation function, which may be expressed as

$$\Delta D_i\left(z,\mu_f^2\right) = \int_0^{\mu_f^2} \frac{dk_\perp^2}{k_\perp^2}\frac{\alpha_s}{2\pi}\left[\int_{z_h}^1 \frac{dx}{x}\sum_{j=q,g} \times \left\{\Delta P_{i\to j}(x,x_B,x_L,k_\perp^2) D_j^h\left(\frac{z_h}{x},\mu_f^2\right)\right\}\right]. \tag{6}$$

In this equation, $\Delta P_{i\to j}$ represents the medium-modified splitting function of parton i into j where a momentum fraction x is left in parton j. The argument $x_L = k_\perp^2/[2P^- p^+ x(1-x)]$ is a momentum fraction defined such that $x_L P^-$ is the formation time of the radiated parton,[1] where the radiated gluon or quark carries away a transverse momentum $k_\perp$, P^- is the incoming momentum of a nucleon in the nucleus, and p is the momentum of the virtual photon. The scale μ_f refers to the hard scale of the process. The medium-modified splitting functions may be expressed as a product of the vacuum splitting function $P_{i\to j}$ and a medium-dependent factor, that is,

$$\Delta\hat{P}_{i\to j} = P_{i\to j}(x)\frac{C_A 2\pi\alpha_s T_{qg}^A(x_B,x_L)}{(k_\perp^2+\langle q_\perp^2\rangle)N_c f_q^A(x_B)}, \tag{7}$$

where C_A, N_c represent the adjoint Casimir and the number of colors. The mean transverse momentum of the soft gluons is represented by the factor $\langle q_\perp^2\rangle$. The term T_{qg}^A represents the quark-gluon correlation in the nuclear medium and depends on the four-point correlator,

$$\langle P|\bar\psi(0)\gamma^- F_\sigma^-(y_2)F^{-\sigma}(y_1)\psi(y)|P\rangle \sim C\langle p_1|\bar\psi(0)\gamma^-\psi(y)|p_1\rangle\langle p_2|F_\sigma^-(y_2)F^{-\sigma}(y_1)|p_2\rangle, \tag{8}$$

where $F_\sigma^-(y_2)$ and $F^{-\sigma}(y_1)$ represent gluon field operators at the locations y_1, y_2 and $\psi(y)$ represents the quark field operator. The above correlation function cannot be calculated from first principles without making assumptions regarding the structure of the medium. The only assumption made is that the color correlation length is small. As a result, one may factorize the four-point function into two separate structure functions, one for the original parton produced in the hard scattering [this is a quark in Eq. (8)] and one for the soft gluon off which the parton scatters in the final state.

While in media with short-distance color correlation lengths such as the atomic nucleus or a QGP with a large Debye mass, this factorization may be generally thought to be true, it may fail at very large jet energies where saturation effects become important. It should also be pointed out that the factorization assumption above falls in the same class as the assumption of independent scattering centers as assumed in the ASW or GLV scheme. In the application of this formalism to RHIC data, we have assumed that the jet energies are not high enough for the onset of saturation effects. Another scenario in which the above factorization may not hold is if there were long-distance color correlations in the QGP, which have been assumed to be absent. If such long-distance correlations were present, then one would have to resort to the definition of more general multiparticle operators [such as the first line in Eq. (8)] and parametrize these in comparison with experimental data.

The entire phenomenology of the medium is incorporated as a model for the expectation of the second set of operators in Eq. (8). This may be characterized in terms of the well-known medium transport coefficient $\hat q(\zeta)$, at location ζ, where

$$\hat q(\zeta) = \frac{4\pi^2\alpha_s C_R}{N_c^2-1}\int\frac{d\xi^+}{2\pi}\frac{d^2\xi_\perp d^2k_\perp}{(2\pi)^2}\exp\left[i\frac{q_\perp^2}{2p^+}\xi^+ - i\vec p_\perp\cdot\vec\xi_\perp\right] \times\langle F_\sigma^{-\cdot}(\zeta+\xi^+/2,\vec\xi_\perp/2)F^{\sigma-}(\zeta-\xi^+/2,-\vec\xi_\perp/2)\rangle. \tag{9}$$

The Casimir C_R depends on the representation of the probe. The transport coefficient is normalized by fitting to one data point, and a model such as a Woods-Saxon distribution for cold matter or 3D hydrodynamic evolution for hot nuclear matter is invoked for its variation with space-time location. The expectation $\langle\,\rangle$ is meant to be taken in the medium under consideration. Any space-time dependence is essentially included in the implied expectation.

Closer inspection of Eq. (9) reveals that it is a function of the jet energy p^+. Note that p^+ is not integrated out. The actual dependence on p^+ depends on the medium in question. In the case of confined nuclear media, or a quark-gluon plasma, the dependence is logarithmic. There is also a logarithmic dependence on the virtuality of the jet which sets in because of radiative corrections to the definition in Eq. (9). Also, as demonstrated in Ref. [59], $\hat q$ may even possess a tensorial structure if the medium is not isotropic. In the calculations of the current manuscript, both the dependence on the energy and virtuality of the jet will be ignored. The medium will be assumed to be isotropic. The values of $\hat q$ quoted should thus be considered as approximations to the full functional form.

Unlike the remaining formalisms, the HT approach is set up to directly calculate the medium-modified fragmentation function and as a result the final distribution of hadrons. This modification to the distribution includes both contributions

[1]Throughout the HT portion of this work, four-vectors will often be referred to using the light-cone convention where $x^\pm = (x^0 \pm x^3)/\sqrt{2}$. For the HT scheme, often $x^+ = (x^0+x^3)/2$ and $x^- = x^0 - x^3$.

coming solely from the medium and those which involve interference between medium-induced and vacuum radiation. The determined constant $\hat{q}$ may be used to calculate the average energy loss encountered by a jet. Other advantages of this approach include a functional difference between the quark and gluon energy-loss kernels, i.e., the difference between the modification as encountered by a quark jet and a gluon jet is not merely assumed to be a ratio of Casimirs, but also depends strongly on the different splitting and fragmentation functions. This formalism offers by far the most straightforward generalization to multiparticle correlations [60] and their modification in the medium.

A disadvantage of this approach at the current state of approximation (similar to the GLV and the ASW but different from the AMY approach) is its neglect of the quark structure function in the medium: as a result, collisions with the medium may not change the flavor of the jet parton; however, this may continue to occur through the splitting kernels. Yet another disadvantage is the restriction to single scattering followed by single radiation in the medium, which makes this formalism more appropriate to thin media. This is partially improved by converting Eq. (7) to an evolution equation as in Ref. [41] which describes the virtuality evolution of the probe in the medium.

As this formalism is originally cast in cold nuclear matter, the applicability of the formalism only depends on there being a short-distance color correlation length in the medium. As a result, it may be used to describe both confined and deconfined matter with the inclusion of an ansatz for the variation of $\hat{q}$ with an intensive property of the medium such as energy density ϵ, entropy density s, or the temperature T and baryon chemical potential μ_B.

B. Opacity expansion: Quenching weights formalism

The path integral approach for the energy loss of a hard jet propagating in a colored medium was first introduced in Ref. [17]. It was later demonstrated to be equivalent to the well-known Baier-Dokshitzer-Mueller-Peigneé-Schiff (BDMPS) approach [14,15] in the limit of multiple scatterings [61]. The current, most widespread variant of this approach developed by numerous authors [21,62] is often referred to as the Armesto-Salgado-Wiedemann (ASW) approach. In this scheme, one incorporates the effect of multiple scattering of the incoming and outgoing partons in terms of a path integral over a path-ordered Wilson line [47].

This formalism assumes a model for the medium as an assembly of Debye screened heavy scattering centers which are well separated in the sense that the mean free path of a jet $\lambda \gg 1/\mu$ the color screening length of the medium [12]. The opacity of the medium $\bar{n}$ quantifies the number of scattering centers seen by a jet as it passes through the medium, i.e., $\bar{n} = L/\lambda$, where L is the thickness of the medium. A hard, almost on-shell, parton traversing such a medium will engender multiple transverse scatterings of order $\mu \ll p^+$. It will, in the process, split into an outgoing parton and a radiated gluon which will also scatter multiply in the medium. The propagation of the incoming (outgoing) partons as well as that of the radiated gluon in this background color field may be expressed in terms of effective Green's functions $[G(\vec{r}_\perp,z;\vec{r}'_\perp,z')$ (for quark or gluon)] which obey the obvious Dyson-Schwinger equation,

$$\begin{aligned} &G(\vec{r}_\perp,z;\vec{r'}_\perp,z') \\ &\quad = G_0(\vec{r}_\perp,z;\vec{r'}_\perp,z') - i\int_z^{z'} d\zeta \int d^2\vec{x}\, G_0(\vec{r}_\perp,z;\vec{x},\zeta) \\ &\qquad \times A_0(\vec{x},\zeta) G(\vec{x},\zeta;\vec{r'}_\perp,z'), \end{aligned} \tag{10}$$

where G_0 is the free Green's function and A_0 represents the color potential of the medium. The solution for the above interacting Green's function involves a path-ordered Wilson line which follows the potential from the location $[\vec{r}_\perp(z'), z']$ to $[\vec{r}_\perp(z), z]$. Expanding the expression for the radiation cross section to order A_0^{2n} corresponds to an expansion up to nth order in opacity.

Taking the high-energy limit and the soft radiation approximation ($x \ll 1$), one focuses on isolating the leading behavior in x that arises from the large number of interference diagrams at a given order of opacity. As a result of the approximations made, one recovers the BDMPS condition that the leading behavior in x is contained solely in gluon rescattering diagrams. This results in the expression for the inclusive energy distribution for gluon radiation off an in-medium produced parton as [63]

$$\begin{aligned} \omega\frac{dI}{d\omega} &= \frac{\alpha_s C_R}{(2\pi)^2\omega^2} 2\mathrm{Re}\int_{\zeta_0}^{\infty} dy_l \int_{y_l}^{\infty} d\bar{y}_l \\ &\quad \times \int d\vec{u} \int_0^{\chi x p^+} d\vec{k} e^{-i\vec{k}\cdot\vec{u} - \frac{1}{2}\int d\zeta n(\zeta)\sigma(\vec{u})} \\ &\quad \times \frac{\partial^2}{\partial y \partial u} \int_{\vec{y}=0=\vec{r}(y_l)}^{\vec{u}=\vec{r}(\bar{y})} \mathcal{D}r e^{i\int d\zeta \frac{\omega}{2}\left(|\dot{\vec{r}}|^2 - \frac{n(\zeta)\sigma(\vec{r})}{i\omega}\right)}, \end{aligned} \tag{11}$$

where, as always, $k_\perp$ is the transverse momentum of the radiated gluon with energy ω, and χ is a factor that introduces the kinematic bound. The vectors $\vec{y}$ and $\vec{u}$ represent the transverse locations of the emission of the gluon in the amplitude and the complex conjugate, whereas y_l and $\bar{y}_l$ represent the longitudinal positions. The density of scatterers in the medium at location ζ is $n(\zeta)$, and the scattering cross section is $\sigma(r)$. In this form, the opacity is obtained as $\int n(\zeta)\,d\zeta$ over the extent of the medium. The Casimir C_R depends on the representation of the jet parton.

Exact analytical expressions for the gluon radiation intensity distribution are rather involved and only yield simple expressions in certain special circumstances. Numerical implementations of this scheme have focused on two separate regimes. In one case, $\sigma(r)$ is replaced with a dipole form $\hat{q}r^2/n(\zeta)$ and one solves the harmonic-oscillator-like path integral. This corresponds to the case of multiple soft scatterings of the hard probe. In the limit of a static medium with a very large length, one obtains the simple form for the radiation distribution

$$\omega\frac{dI}{d\omega} \simeq \frac{2\alpha_s C_R}{\pi} \begin{cases} \sqrt{\frac{\omega_c}{2\omega}} & \text{for } \omega < \omega_c, \\ \frac{1}{12}\left(\frac{\omega}{\omega_c}\right)^2 & \text{for } \omega > \omega_c. \end{cases} \tag{12}$$

Where $\omega_c = \int d\zeta\, \zeta \hat{q}(\zeta)$ is called the characteristic frequency of the radiation. Up to constant factors, this is equal to mean energy lost in the medium ($\langle E \rangle$), i.e., $\omega_c \simeq 2\langle E \rangle/(\alpha_s C_R)$. In the other extreme, one expands the exponent as a series in $n\sigma$; keeping only the leading-order term corresponds to the picture of gluon radiation associated with a single scattering. In this case, the gluon emission intensity distribution has been found to be rather similar, once scaled with the characteristic frequency appropriate for this situation. For dynamical medium of finite extent, the characteristic frequency and the overall mean transverse momentum gained by the jet $\langle \hat{q} L \rangle$ will have to be estimated based on an ansatz for the space-time distribution of the transport parameter $\hat{q}$.

Because of the soft limit used, i.e., $\omega \to 0$, multiple gluon emissions are required for a substantial amount of energy loss. Each such emission at a given opacity is assumed independent, and a probabilistic scheme is set up wherein the jet loses an energy fraction ΔE in n tries with a Poisson distribution [21],

$$P_n(\Delta E) = \frac{e^{-\langle I \rangle}}{n!} \Pi_{i=1}^{n} \left[\int d\omega_i \frac{dI}{d\omega_i} \right] \delta \left(\Delta E - \sum_{i=1}^{n} \omega_i \right), \tag{13}$$

where $\langle I \rangle$ is the mean number of gluons radiated per coherent interaction set. Summing over n gives the probability $P(\Delta E)$ for an incident jet to lose a momentum fraction ΔE due to its passage through the medium. This is then used to model a medium-modified fragmentation function by shifting the energy fraction available to produce a hadron (as well as accounting for the phase space available after energy loss):

$$\tilde{D}(z, Q^2) = \int_0^1 d\Delta E\, P(\Delta E) \frac{D\left(\frac{z}{1-\Delta E}, Q^2\right)}{1 - \Delta E}. \tag{14}$$

This modified fragmentation function is then used in a factorized formalism as in Eq. (5) to calculate the final hadronic spectrum.

In marked contrast to other approaches, this scheme presents the advantage of easy interpolation between the cases of few hard scatterings and multiple soft scatterings and is thus applicable to both thin and thick media. The inclusion of the zero opacity term makes this the only formalism, to date, that includes interference between vacuum radiation and radiation induced by multiple soft scattering in the medium. It suffers from the disadvantage of having approximated the medium in terms of heavy static scattering centers. As a result, elastic energy loss is vanishing in this scheme. As the formalism is set up to calculate the energy-loss probability of the leading hard parton, estimation of the change in the distribution of final associated (subleading) hadrons or partons is not straightforward.

Along with the HT formalism, this approach also neglects any flavor changing scatterings in the medium. Also similar with HT is the treatment of both confined and deconfined matter on the same footing: one essentially makes an ansatz for the variation of $\hat{q}$ with an intensive variable of the medium, e.g., ϵ, s, T, μ_B.

C. Finite temperature field theory formalism

In this scheme, often referred to as the Arnold-Moore-Yaffe (AMY) approach the energy loss of hard jets is considered in an extended medium in equilibrium at asymptotically high temperature $T \to \infty$. Owing to asymptotic freedom, the coupling constant $g \to 0$ at such high temperatures, and a power counting scheme emerges from the ability to identify a hierarchy of parametrically separated scales $T \gg gT \gg g^2T$, etc. In this limit, it then becomes possible to construct an effective field theory of soft modes, i.e., $p \sim gT$ by summing contributions from hard loops with $p \sim T$, into effective propagators and vertices [64].

One assumes a hard on-shell parton, with energy several times that of the temperature, traversing such a medium, and undergoing soft scatterings with momentum transfers $\sim gT$ off other hard partons in the medium. Such soft scatterings induce collinear radiation from the parton, with a transverse momentum of the order of gT. The formation time for such collinear radiation $\sim 1/(g^2T)$ is of the same order of magnitude as the mean free time between soft scatterings [51]. As a result, multiple scatterings of the incoming (outgoing) parton and the radiated gluon need to be considered to get the leading-order gluon radiation rate. One essentially calculates the imaginary parts of infinite-order ladder diagrams such as those shown in Fig. 3; this is done by means of integral equations [65].

The imaginary parts of such ladder diagrams yield the $1 \to 2$ decay rates of a hard parton into a radiated gluon and another parton. These decay rates are then used to evolve hard quark and gluon distributions from the initial hard collisions, when they are formed, to the time when they exit the medium, by means of a set of coupled Fokker-Planck–like equations for quarks, antiquarks, and gluons [22,33,53], which may be written schematically as

$$\frac{dP_j(p,t)}{dt} = \sum_{ab} \int dk \left[P_a(p+k,t) \frac{d\Gamma^a_{jb}(p+k,p,t)}{dk\, dt} - P_j(p,t) \frac{d\Gamma^j_{ab}(p,k,t)}{dk\, dt} \right]. \tag{15}$$

In this equation, $j = q, \bar{q}, g$, and we sum over all relevant partonic processes for each evolution equation. In contrast to all other schemes, this approach also includes the absorption of thermal gluons as well as quark-antiquark pair annihilation and creation.

The initial jet distributions are taken from a factorized hard scattering cross section as in Eq. (5). In the limit of single scattering, these rates may be taken directly from the corresponding Gunion-Bertsch cross sections [66] for an on-shell parton to radiate a gluon on soft scattering with another in-medium parton.

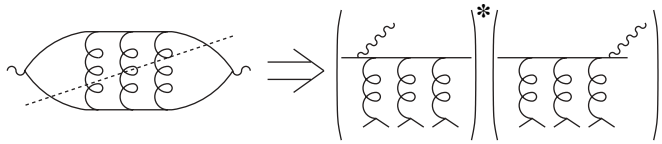

FIG. 3. Ladder diagram evaluated in the AMY formalism.

The final hadron spectrum at high p_T is obtained by the fragmentation of jets in the vacuum after their passing through the medium. In this approach one calculates the medium-modified fragmentation function by convoluting the vacuum fragmentation functions with the hard parton distributions, at exit, to produce the final hadronic spectrum [53],

$$\tilde{D}_j^h(z,\vec{r}_\perp,\phi) = \sum_{j'} \int dp_{j'} \frac{z'}{z} D_{j'}^h(z') P(p_{j'}|p_j,\vec{r}_\perp,\phi), \quad (16)$$

where the sum over j' is the sum over all parton species. The two momentum fractions are $z = p_h/p_j$ and $z' = p_h/p_{j'}$, where p_j and $p_{j'}$ are the momenta of the hard partons immediately after the hard scattering and prior to exit from the medium, and p_h is the final hadron momentum. $P(p_{j'}|p_j,\vec{r}_\perp, \phi)$ represents the solution to Eq. (15), which is the probability of obtaining a given parton j' with momentum $p_{j'}$ when the initial condition is a parton j with momentum p_j. The above integral depends implicitly on the path taken by the parton and the medium profile along that path, which in turn depends on the location of the origin $\vec{r}_\perp$ of the jet, its propagation angle ϕ with respect to the reaction plane. Therefore, one must convolve the above expression over all transverse positions $\vec{r}_\perp$ and directions ϕ.

The use of an effective theory for the description of the medium and the propagation of the jet makes this approach considerably more systematic than the two previous approaches: the properties of both the jet and the medium are described using the same hierarchy of scales. It remains the only approach to date that naturally includes partonic feedback from the medium, i.e., processes where a thermal quark or gluon may be absorbed by the hard jet.[2] In contrast to ASW and HT, this approach also includes flavor changing interactions in the medium. Elastic energy loss may also be incorporated within the same basic formalism [67]. Note that AMY assumes a thermalized partonic medium and neglects the quenching of jets in the confined sector. In addition, interference between medium and vacuum radiations is not yet considered.

The use of hard-thermal-loop (HTL) effective theory to describe both the jet propagation in the medium and the properties of the medium itself does suffer from one caveat: this scheme approximates the bulk structure of the medium as a weakly coupled plasma of quarks and gluons. The perturbative estimates of the energy density ϵ differs from the $\epsilon(T)$ obtained from lattice calculations (at $3T_c \geqslant T \gtrsim T_c$). The η/s required to reproduce the observed magnitude of elliptic flow in viscous fluid dynamical simulations is at least a factor of 2 lower than perturbative results. The application of such a scheme to the modification of hard jets involves an aspect of phenomenology in which the coupling constant is used as a fit parameter.

D. Geometry and discussion of the different schemes

As mentioned previously, all parameters of our hydrodynamic evolution [30] have been fixed by a fit to the soft sector (elliptic flow, pseudorapidity distributions, and low-p_T single-particle spectra), therefore providing us with a fully determined medium evolution for the hard probes to propagate through. The hydrodynamic calculation provides a time-evolution of the temperature, energy density, flow velocity, and QGP to hadron gas fraction within all hydrodynamic cells composing the medium through which the hard probes evolve. The incorporation of this information within the different jet energy-loss schemes is described in the following subsections.

The mean impact parameters for the different evolution sets have been set to $b = 2.4$, 4.5, 6.3, and 7.5 fm, corresponding to 0–5, 10–15, 15–20, and 20–30% centrality, respectively. These values were estimated via the number of nucleon-nucleon binary collisions and the number of participant nucleons in Ref. [7]. In this work, the focus will lie on the two extreme centrality bins in the list above: the 0–5% bin and the 20–30% bin. All the RFD calculations utilized here have an initial thermalization time of $\tau_0 = 0.6$ fm/c. Any values of parameters, such as $\hat{q}$, that are dependent on the bulk properties of the medium will be quoted at this time.

All three energy-loss schemes are sensitive to certain bulk properties of the evolving matter: while in the AMY formalism this is decidedly the temperature, the relation between $\hat{q}$ and the intensive variables of the medium in the HT and ASW formalisms is unspecified. Traditionally, the $\hat{q}$ in the ASW scheme has been related to the the energy density ϵ via $\epsilon^{3/4}$, while the $\hat{q}$ in the HT scheme has been scaled either with the temperature T via T^3 or the entropy density s of the local medium. In the analysis presented in this paper, we maintain this methodology; however, some surprising results of scaling the ASW $\hat{q}$ with T^3 and the HT $\hat{q}$ with $\epsilon^{3/4}$ will also be presented.

The scaling of $\hat{q}$ with $\epsilon^{3/4}$, T^3, or s will by construction yield identical results for a QGP with an ideal gas equation of state: $\epsilon = 3p$. However, for a more realistic nonideal EOS as used in our hydrodynamic calculation, the value of $\hat{q}$ will be affected by the choice of scaling variable, in particular if energy loss persists to temperatures below T_C. Figure 4 investigates the deviations from the ideal gas scaling by plotting the normalized time evolution of temperature T^3, energy density $\epsilon^{3/4}$, and entropy density s. As can be seen, after 2 fm/c the curves start to deviate from the ideal gas power-law behavior and start to show differences for times later than $\tau = 3$ fm/c. The first-order phase transition contained in our equation of state results in a striking difference between the temperature and the energy- or entropy-density scaling at the critical temperature and below. We note that the *proper* scaling law for $\hat{q}$ is *a priori* not known, even though we see no reason why it should not be calculable in QCD.

1. Higher twist

In the preceding section, the medium modification of the final fragmentation function in the HT formalism was shown to be dependent on the transport coefficient $\hat{q}$ [see Eq. (9)]. In the evolving system formed in the collision of two nuclei, this transport coefficient has both a space and time dependence [i.e., $\hat{q}(x, y, z, \tau)$]. Phenomenologically, this dependence is

[2] While an attempt to include such effects in the HT formalism have been made in Ref. [68], these remain as phenomenological extensions and have not been included in this manuscript.

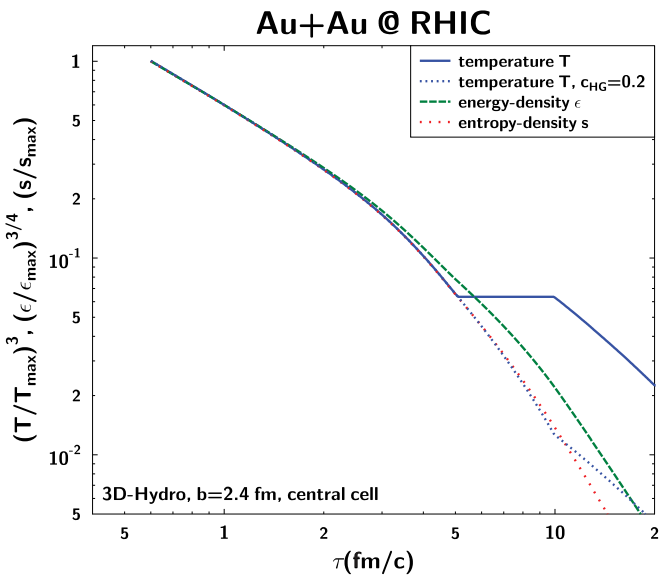

FIG. 4. (Color online) Time evolution of temperature T^3, energy density $\epsilon^{3/4}$, and entropy density s as a function of time τ in the central cell of the hydrodynamic evolution for Au + Au collisions at RHIC. All curves are normalized to their maximum values at $\tau = 0.6$ fm/c.

taken to scale with some intensive variable of the medium, in this case, the dimensionally equivalent quantities of T^3 or the entropy density s, i.e.,

$$\hat{q}(x, y, z, \tau) = \hat{q}_0 \frac{\gamma_\perp(x, y, z, \tau) T^3(x, y, z, \tau)}{T_0^3} \times [R(x, y, z, \tau) + c_{\rm HG}\{1 - R(x, y, z, \tau)\}], \quad (17)$$

where $T(x, y, z, \tau)$, $\gamma_\perp(x, y, z, \tau)$, and $R(x, y, z, \tau)$ represent the temperature, flow transverse to the jet, and the volume fraction in the plasma phase at the space-time point x, y, z, τ. It is this information that is extracted from the RFD simulation. Though the RFD simulations start at $\tau = 0.6$ fm/c, the values of T and $\gamma_\perp$ at $\tau = 0.6$ fm/c are extrapolated as constants to $\tau = 0$, which represents the time of the initial hard scatterings (the effect of different extrapolation schemes involving linearly rising or dropping values of $\hat{q}$ as $\tau \to 0$ has been found to be rather small and will not be studied in this effort). The factors $\hat{q}_0$,T_0 represent the maximum $\hat{q}$ and temperature achieved in the simulation; in this particular version of RFD, $T_0 = 0.405$ GeV and $\hat{q}_0$ is a fit parameter adjusted to fit one data point of the R_{AA}, at one centrality.

The factor $c_{\rm HG}$ may be interpreted in two ways. In essence, it accounts for the fact that the quenching in the hadronic phase may not be as effective as that in the partonic phase at the same temperature. Since the entropy density in a given phase is proportional to T^3 with the constant of proportionality demonstrating a weak dependence on temperature, $c_{\rm HG}$ may be tuned to convert the scaling of $\hat{q}$ with T^3 into a scaling with s. This is approximately achieved with a $c_{\rm HG} \sim 0.2$, as can be seen in Fig. 4. Unless specified otherwise, this is the value used for $c_{\rm HG}$ in all the plots in this paper. Thus $c_{\rm HG}$ is not a fit parameter and is not tuned to fit any experimental data point. It has only three possible values: $c_{\rm HG} = 0$ which corresponds to no quenching in the hadronic phase, $c_{\rm HG} = 1$ which corresponds to exact scaling of $\hat{q}$ with T^3, and $c_{\rm HG} = 0.2$ which corresponds to approximate scaling of $\hat{q}$ with s.

Given a choice of $c_{\rm HG}$ and the overall fit parameter $\hat{q}_0$, we use Eq. (7) to calculate a medium-modified fragmentation function; then Eq. (5) is used to compute the total cross section and the nuclear modification factor R_{AA}. The overall fit parameter $\hat{q}_0$ is tuned to fit one experimental data point, at one centrality and p_T. For the current effort, the fit parameter is set by requiring that the R_{AA} at $p_T = 10$ GeV in the most central event (0–5% centrality) is 0.2. With the value of $\hat{q}_0$ and $c_{\rm HG}$ fixed, the variation of R_{AA} as a function of p_T (integrated over or with respect to the angle with the reaction plane) and centrality of the collision are predictions.

2. ASW

As in the previous case, we have to formulate the energy-loss problem for a dynamical medium in which the transport coefficient $\hat{q}$ acquires a space and time dependence. As done in previous calculations within the ASW formalism, we use a scaling with the local energy density $\epsilon^{3/4}$ along the path $\xi = (x(\tau), y(\tau), z(\tau), \tau)$ of a parton as

$$\hat{q}(\xi) = 2K\epsilon^{3/4}(\xi). \quad (18)$$

This scaling of $\hat{q}$ is assumed to be valid in both the partonic and hadronic phases. The precise form of the path ξ is determined once the hard initial vertex (x_0, y_0) in the transverse plane, the outgoing parton rapidity η, and the angle of the parton with the reaction plane ϕ are specified. The parameter K in Eq. (18) accounts for the uncertainty in the selection of α_s and possible nonperturbative effects increasing the quenching power of the medium (see discussion in Ref. [69]).

Given this space-time dependence of the transport coefficient along a parton trajectory, the energy-loss probability distribution can be computed from the two line integrals

$$\omega_c(\mathbf{r_0}, \phi) = \int_0^\infty d\xi \xi \hat{q}(\xi) \quad \text{and} \quad \langle \hat{q}L \rangle(\mathbf{r_0}, \phi) = \int_0^\infty d\xi\, \hat{q}(\xi). \quad (19)$$

Here, ω_c is the characteristic gluon frequency, setting the scale of the energy-loss probability distribution [see expression (12)], and $\langle \hat{q}L \rangle$ is a measure of the path length, weighted by the local quenching power. Analogous to the overall fit parameter $\hat{q}_0$ in the HT case, the parameter K is fit to one data point of the R_{AA}, at one centrality.

For times prior to $\tau = 0.6$ fm/c, i.e., the starting point of the RFD simulation, we neglect any medium effects, i.e., assume $\hat{q} = 0$. Note that for a purely radiative energy-loss model, where the average energy loss grows quadratically with path length in a constant medium, the effect of initial time dynamics is systematically suppressed, and no strong dependence of the energy loss on variations of the initial time is observed.

Using a dynamical scaling law [49], ω_c and $\langle \hat{q} \rangle$ can then be mapped onto a static equivalent scenario. Using the relation $R = 2\omega_c^2/\langle \hat{q}L \rangle$ as an input, we then determine $P(\Delta E)$ using the numerical results from Ref. [21] and compute the

medium-modified fragmentation function from Eq. (14). The resulting expression (valid for a single path) must then be averaged over the whole geometry with a weight corresponding to the probability of finding an initial hard vertex at (x_0,y_0).

3. AMY

The strength of the transition rate in pQCD is controlled by the strong coupling constant $\alpha_s(T)$, temperature T, and the flow parameter $\vec{\beta}$ (the velocity of thermal medium) relative to the jet's path. The value for the coupling constant used (along with the assumption of a thermalized partonic medium) may be related to the transport coefficient $\hat{q}$ as derived from computations in HT or ASW by either a direct computation of the operator product in Eq. (9), or a computation of the mean transverse momentum squared per unit length as gained by a jet that propagates through the medium without radiation.

In a 3D expanding medium, the transition rate is first evaluated in the local frame of the thermal medium, then boosted into the laboratory frame,

$$\left.\frac{d\Gamma(p,k,t)}{dk\,dt}\right|_{\text{lab}} = (1-\vec{v}_j\cdot\vec{\beta})\left.\frac{d\Gamma(p_0,k_0,t_0)}{dk_0\,dt_0}\right|_{\text{local}}, \quad (20)$$

where $k_0 = k(1-\vec{v}_j\cdot\vec{\beta})/\sqrt{1-\beta^2}$ and $t_0 = t\sqrt{1-\beta^2}$ are momentum and the proper time in the local frame. As jets propagate in the medium, the temperature and the flow parameters depend on the time and the positions of jets, and the 3D hydrodynamical calculation [30] is utilized to determine the temperature and flow profiles. The energy-loss mechanism is applied at time $\tau_0 = 0.6$ fm/c, when the medium reaches thermal equilibrium, and switched off when the medium reaches the hadronic phase.

IV. APPLICATION TO RHIC DATA

In the preceding sections, a description of the theoretical setup underlying each of the three schemes as well as the phenomenological connection between them and the RFD simulations was expounded upon. In this section, we present the results of our numerical calculations. The primary quantity of interest will be the nuclear modification factor R_{AA} defined as

$$R_{AA} = \frac{\frac{d\sigma^{AA}(b_{\min},b_{\max})}{dy\,d^2p_T}}{\int_{b_{\min}}^{b_{\max}} d^2b\,T_{AA}(b)\frac{d\sigma^{pp}(p_T,y)}{dy\,d^2p_T}}, \simeq \frac{\frac{d\sigma^{AA}(\langle b\rangle)}{d^2b\,dy\,d^2p_T}}{T_{AA}(\langle b\rangle)\frac{d\sigma^{pp}(p_T,y)}{dy\,d^2p_T}}, \quad (21)$$

where T_{AA} represents the nuclear overlap function, which is proportional to the number of binary collisions at the mean impact parameter $\langle b\rangle$. The mean impact parameter for a given range of centrality is essentially set by the RFD simulation used to calculate the soft observables. The R_{AA} is calculated both integrated as defined above or as function of the angle with respect to the reaction plane.

The range of p_T of the detected hadron is set high enough for the applicability of pQCD. In this paper, the lower bound is set at $p_T = 6$ GeV. This choice is essentially dictated by the regime where recombination [70] begins to contribute to the yield. The upper limit is set at $p_T = 20$ GeV, which represents the highest p_T for which experimental data exist. The focus in this paper will essentially be on two different centralities: one with $\langle b\rangle = 2.4$ fm which represents the rather central collisions with a centrality in the range of 0–6%, and a somewhat more peripheral event with a $\langle b\rangle = 7.5$ fm which corresponds to the 20–30% range of centrality.

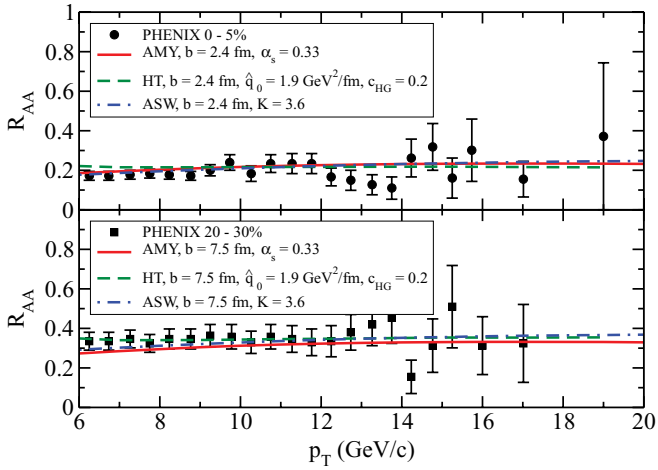

FIG. 5. (Color online) Nuclear modification factor R_{AA} in Au-Au collisions at 0–5% and 20–30% centralities calculated in the ASW, HT, and AMY approaches compared with data from PHENIX [71].

Figure 5 shows the nuclear modification factor R_{AA} as a function of p_T in Au-Au collisions at 0–5% (top) and 20–30% (bottom) centralities calculated in the ASW, HT, and AMY approaches compared with data from PHENIX [71]. The parameters for the respective calculations are fixed to one data point in the 0–5% centrality calculation; the dependence on p_T and centrality of the nuclear collision are then predictions by the respective energy-loss calculations. As can be seen, the parameters for all three approaches (initial maximal value for the transport coefficient $\hat{q}_0$ or coupling constant α_s in the AMY case) can be adjusted such that the approaches are able to describe the centrality dependence of the nuclear modification factor reasonably well. For a gluon jet, the values are $\hat{q}_0 \approx 4.3$ GeV^2/fm for the HT approach $\hat{q}_0 \approx 18.5$ GeV^2/fm for the ASW formalism, and $\alpha_s \approx 0.33$ for the AMY approach which can be converted into a value of $\hat{q}_0 \approx 4.1$ GeV^2/fm. While values of $\hat{q}_0$ have been presented up to the first decimal point, one should note that the error involved is never less than the experimental error (see Sec. V for further discussion on this issue). Beyond this, there remain the usual uncertainties related to using a leading-order hard scattering cross section, e.g., the choice of the appropriate scale for the structure and fragmentation functions. Additional sources of error in the estimations of $\hat{q}$ arise from the set of approximations used in each of the formalisms to reduce the functional dependence on the properties of the medium down to one parameter.

The reader will note a somewhat smaller value of $\hat{q}_0$ quoted for the HT formalism in Fig. 5. Since the HT approach was originally developed for DIS on a large nucleus, it has become

customary to quote the value of $\hat{q}_0$ for a quark which is always the produced hard parton in DIS (see Refs. [45,46]). Besides this difference, there remain various caveats associated with this value of $\hat{q}$ which have been discussed in Sec. III [in particular, see the discussion surrounding Eq. (9)].

For the case of the ASW formalism, we have used the relationship [72]

$$\hat{q}_0 = 2K\epsilon_0^{3/4} \tag{22}$$

to convert the parameter K in the ASW approach to $\hat{q}_0$. In a previous estimate using this formalism [69], the value of $\hat{q}_0$ was quoted to be somewhat lower. This is simply due to the earlier time $\tau_0 = 0.6$ fm/c at which $\hat{q}_0$ is being quoted in the current manuscript. In Ref. [69], τ_0 was set to 1 fm/c.

In AMY, the relationship between $\hat{q}$ and the coupling α_s reads

$$\hat{q} = \frac{C_A g^2 T m_D^2}{2\pi} \ln \frac{q_\perp^{\max}}{m_D}, \tag{23}$$

where $q_\perp^{\max}$ is the largest transverse momentum relevant for the collinear emission. One estimate is that $(q_\perp^{\max})^2 \approx ET$, where E is the energy of the jet, and T the temperature. Evaluating the above expression for three quark flavors, $\alpha_s = 0.33$, a temperature of 0.4 GeV, and a jet energy of 20 GeV, one obtains $\hat{q} = 4.1$ GeV^2/fm. Even though this formulation is only logarithmic in the jet energy, it is, however, more suggestive than precise [73]. Note that the ASW value for $\hat{q}_0$ at $\tau = 0.6$ fm/c and $\epsilon_0 = 55$ GeV/fm^3 lies a factor of 3.6 higher than the Baier estimate for an ideal QGP, $\hat{q} \approx 2\epsilon^{3/4}$ [72], while the AMY estimate is in line with that from Baier, and the HT calculation lies about a factor of 1.6 below that value.

The large difference in $\hat{q}_0$ values between HT, AMY, and ASW has been pointed out previously. However, our calculation shows for the first time that this difference is not due to a different treatment of the medium or initial state. Note that the numbers quoted here reflect the different medium scaling laws referred to as being the natural choices for the respective approaches, namely, temperature scaling for AMY, energy-density scaling for ASW, and entropy-density scaling for HT, as discussed in the previous section. If we choose to perform the jet energy-loss calculation with temperature $\sim T^3$ scaling for all three approaches, we find values for $\hat{q}_0$ being 10 GeV^2/fm for ASW, 2.3 GeV^2/fm for HT and 4.1 GeV^2/fm for AMY. Likewise, if we employ energy-density scaling $\sim\epsilon^{3/4}$, we find $\hat{q}_0 = 18.5$ GeV^2/fm for ASW and $\hat{q}_0 = 4.5$ GeV^2/fm for HT (the AMY calculation can only be performed utilizing temperature scaling). Both ASW and HT consistently show a rise of a factor of 2 in $\hat{q}_0$ when switching from temperature scaling to energy-density scaling. The different values for $\hat{q}_0$ in the different schemes with different choices of scaling with T, s, and $\epsilon^{3/4}$ are presented in Table I.

We find that slight differences appear between the approaches when R_{AA} is studied as a function of azimuthal angle. This can be seen in Fig. 6, where R_{AA} is plotted as a function of azimuthal angle at $p_T = 10$ GeV/c and $p_T = 15$ GeV/c for all three approaches in the 20–30% centrality bin. Figure 7 shows the same calculation, but with all curves normalized by their respective azimuthally averaged R_{AA}; we observe that for the p_T bins chosen, the AMY and HT calculations exhibit the same peak-to-valley ratio and shape, whereas the ASW calculation shows a more pronounced difference between in-plane and out-of-plane emission. The azimuthal spread is insensitive to variation of the transverse momentum, which is manifest in the comparison between the solid ($p_T = 10$ GeV/c) and the dashed ($p_T = 15$ GeV/c) lines.

TABLE I. Values of $\hat{q}_0$ defined as the $\hat{q}$ at $\tau = \tau_0 = 0.6$ fm/c in the cell at $\vec{r} = 0$ of the 0–5% centrality event, in the different energy-loss schemes. Also presented is the variation of $\hat{q}_0$ with different choices of scaling of $\hat{q}(\vec{r},\tau)$ with different local intensive properties of the medium; where $T(\vec{r},\tau)$ is the temperature, $\epsilon(\vec{r},\tau)$ the energy density, and $s(\vec{r},\tau)$ the entropy density at location $(\vec{r},\tau)$ in the RFD simulation. Given the model of the medium in AMY, $\hat{q}$ may only be calculated as a function of T [see Eq. (23)], hence the entries corresponding to ϵ and s scaling are left blank. Calculations in the ASW scheme with $\hat{q}$ scaled with s have not yet been performed, so the entry for s scaling has been left blank.

$\hat{q}(\vec{r},\tau)$ scales as	$\hat{q}_0$ (GeV^2/fm)		
	ASW	HT	AMY
$T(\vec{r},\tau)$	10	2.3	4.1
$\epsilon^{3/4}(\vec{r},\tau)$	18.5	4.5	
$s(\vec{r},\tau)$		4.3	

To further quantify the difference between the three approaches, we calculate the ratio of the out-of-plane R_{AA} over the in-plane R_{AA} as a function of transverse momentum; this is shown in Fig. 8. We find that AMY and HT exhibit the same peak-to-valley ratio throughout the entire range of transverse momenta, even though the absolute values for R_{AA} differ by approximately 10%. The ASW calculation systematically shows a stronger azimuthal dependence than the HT and AMY calculations, the cause of which will require a more detailed analysis to determine.

Note, however, that the agreement in the peak-to-valley ratio for AMY and HT does not translate into these approaches being identical in terms of the in-plane and out-of-plane R_{AA}

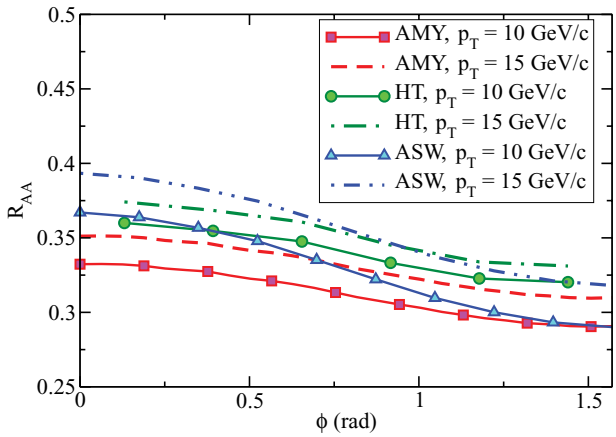

FIG. 6. (Color online) R_{AA} as a function of azimuthal angle at $p_T = 10$ and 15 GeV/c for all three approaches in the 20–30% centrality bin.

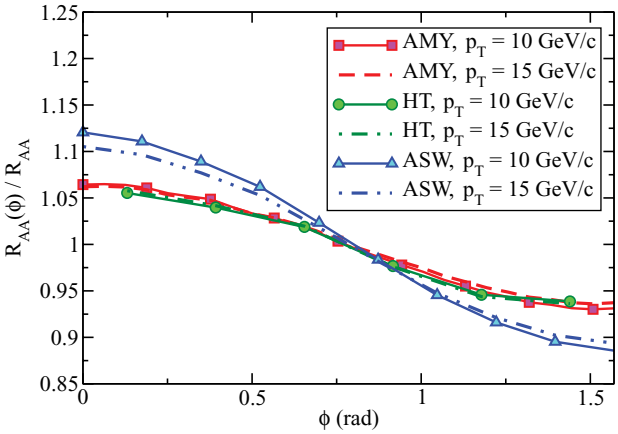

FIG. 7. (Color online) Same as Fig. 6, but normalized by the azimuthally averaged value of R_{AA} for the respective calculations.

values vs p_T: Fig. 9 shows that systematic differences on the order of 15% exist between all three approaches in the absolute value of R_{AA} at fixed azimuthal angle as a function of p_T.

To investigate the spatial response of the jet energy-loss schemes to the medium, we define the following quantity,

$$P(x, y) = \frac{T_{AB}(x, y) R_{AA}(x, y)}{\int dx\, dy\, T_{AB}(x, y) R_{AA}(x, y)}, \tag{24}$$

where the local position-dependent nuclear suppression factor $R_{AA}(x, y)$ is weighted with the nuclear overlap probability function $T_{AB}(x, y)$. Figure 10 shows $P(x, y = 0)$ as a function of x for a quenched jet moving in the positive x direction through the center of the medium ($y = 0$).

Integrating the quantity $P(x, y)$ over y yields the escape probability of a hadron with a transverse momentum between 6 and 8 GeV/c originating from a quenched jet moving in the positive x direction in the transverse plane as a function of of its production vertex along the x axis:

$$P(x) = \int dy P(x, y). \tag{25}$$

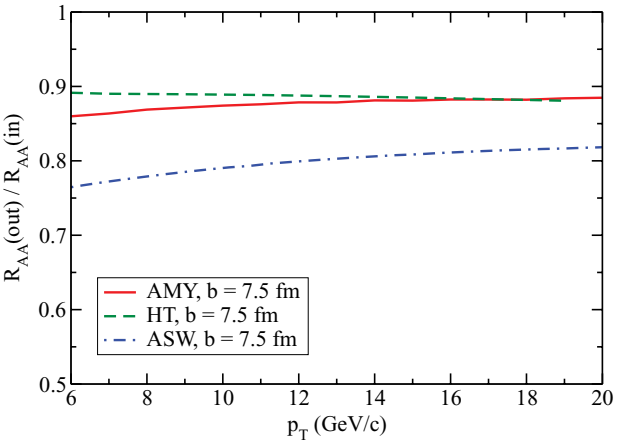

FIG. 8. (Color online) Ratio R_{AA} for out-of-plane vs in-plane emission as a function of p_T at $b = 7.5$ fm impact parameter for all three approaches.

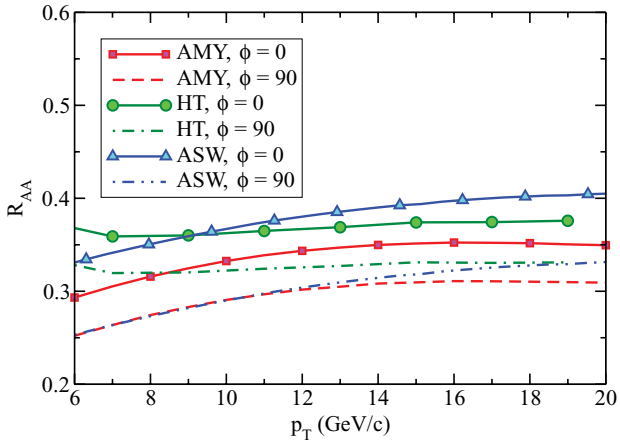

FIG. 9. (Color online) R_{AA} for out-of-plane vs in-plane emission as a function of p_T at $b = 7.5$ fm impact parameter for all three approaches.

The result is shown in Fig. 11. It is remarkable how well the three different approaches agree with each other in this quantity. Since the same hard scattering probability was used as input in all three cases, the agreement in $P(x)$ really shows that all three approaches yield the same suppression factor as a function of production vertex of the hard probe; i.e., they probe the density of the medium in the same way.

V. NORMALIZATION AND FURTHER COMPARISON WITH DATA

As we have seen in the previous section, there do exist noticeable differences in the R_{AA} as a function of the azimuthal angle between the three approaches. A comparison with experimental data for this particular observable would thus constitute an important experimental input and possibly serve as a discriminator. Recently, data for R_{AA} vs the reaction plane have become available in the $p_T = 5$–8 GeV region [74]. Unfortunately this p_T range, which in terms of the data will

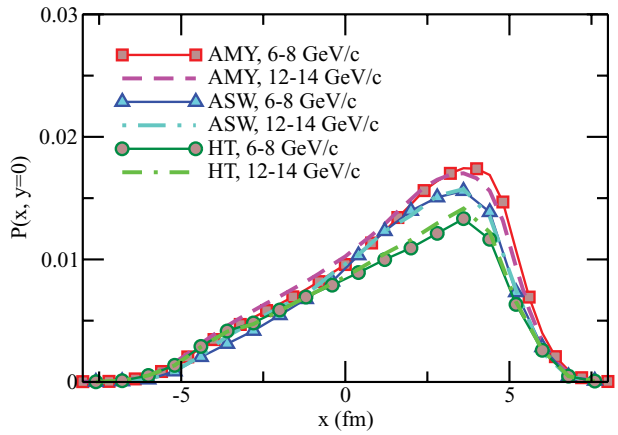

FIG. 10. (Color online) Survival probability $P(x, y)$ of a hadron with 6–8 or 12–14 GeV/c transverse momentum moving along the positive x axis through the center of the medium ($y = 0$) in the transverse plane as a function of x.

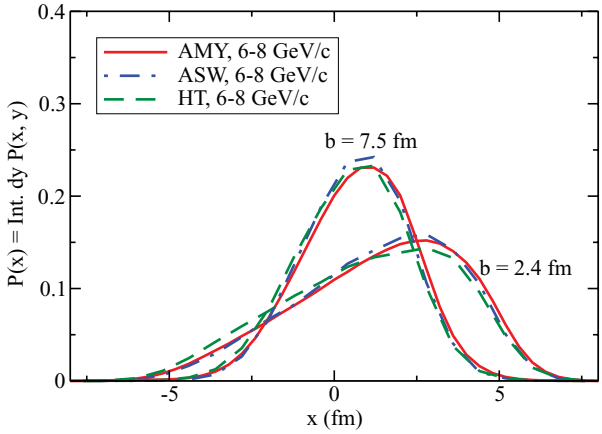

FIG. 11. (Color online) Escape probability of a hadron with 6–8 GeV/c transverse momentum moving along the positive x axis in the transverse plane as a function of x.

be dominated by the lower p_T boundary, still sits in the region in which particle production is significantly influenced by parton recombination as the hadronization mechanism [70,75]. Since we regard $p_T = 6$ GeV as the lower limit of the applicability of jet-quenching calculations, a comparison may not be completely out of place, but it would carry large uncertainties with it.

However, the data from run-2 of the PHENIX Collaboration [74], which was used to deduce the R_{AA} vs the reaction plane, demonstrate an integrated R_{AA} of 0.41 ± 0.03(stat) ± 0.06(sys) in the 20–30% centrality events, in noticeable contrast to the value of $0.35 \pm \sim 0.04$(stat) $\pm \sim 0.03$(sys) as seen in Fig. 5 from the run-4 data set. While the two data sets agree within systematic errors, the discrepancy between the two is too large for a meaningful comparison of our calculation, which was fit to the run-4 data set.

An estimate of the variation of the fit parameters required to encompass both data sets leads to differences of the order of 20–40% in $\hat{q}$. Plotted in Fig. 12 are the predictions for the R_{AA} vs reaction plane for the standard values of the fit parameters obtained from the comparison with the run-4 data

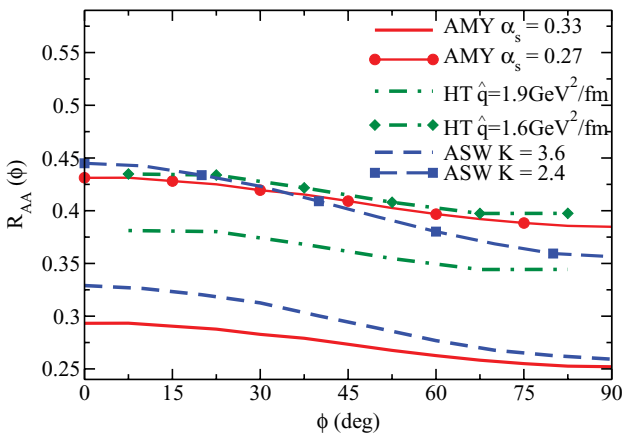

FIG. 12. (Color online) R_{AA} vs reaction plane in the 20–30% centrality event at $p_T = 6$ GeV for different choices of the single fit parameters $\hat{q}$, K, α_s.

set in Fig. 5. Also plotted are readjusted plots for the R_{AA} vs the reaction plane, where the single fit parameters in each of the models was tuned such that the integrated R_{AA} in the 20–30% centrality bin achieved a value of 0.41. The new values of the fit parameters (included in the figure) are $\hat{q} = 1.6$ GeV^2/fm for the HT, $K = 2.4$ for the ASW, and $\alpha_s = 0.27$ for the AMY calculations. One should note that a simple renormalization of our R_{AA} vs ϕ curves to the data would not be appropriate, since the value of $\hat{q}$ affects the magnitude of the azimuthal spread.

A detailed and meaningful theory-experiment comparison, encompassing different data sets as well as their respective statistical and systematic errors in a proper fashion, will require a sophisticated statistical analysis beyond the scope and aim of the work presented here. Such an analysis has been demonstrated for one particular theory calculation of inclusive R_{AA} vs p_T compared to one experimental data set in Ref. [76]. The feasibility of extending such an analysis to multiple data sets, observables, and theory calculations has yet to be determined.

VI. SUMMARY AND CONCLUSION

In summary, we have calculated the modification of hard jets in a 3D hydrodynamic medium in three different approaches, which were constrained to use the same initial structure functions, the same final vacuum fragmentation functions, the same nuclear geometry, and identical 3D evolution of the produced dense matter. In this first unified attempt to understand jet modification in dense matter, the focus was restricted to single inclusive observables. The nuclear modification factor [Eq. (21)] was computed as a function of the transverse momentum and centrality of collision, as well as the angle with respect to the reaction plane. This was followed by a more detailed, though purely theoretical, analysis of jet origin distribution for the R_{AA} as a function of the reaction plane, as well as the R_{AA} for jet origins restricted to lie on a narrow belt on the reaction plane.

In the comparisons above, both the HT and the ASW schemes were simplified to the point that all predictions depended on only one tunable parameter: this is the $\langle FF \rangle$ correlator in the HT approach and the K parameter in the ASW approach. In the most rigorous formulation of AMY, there exist no free parameters except for the temperature; this, however, has already been specified by the RFD simulation. In the phenomenological application of the AMY approach used here, the strong coupling constant is treated as a parameter; it has, thus, been disassociated from the temperature.

These single free parameters from all three approaches were tuned to fit one data point, usually chosen as the integrated R_{AA} at 8 GeV in the 0–5% centrality events. The data used for this comparison as shown in Fig. 5 were taken from the PHENIX run-4 data set [71]. Our comparison shows that under identical conditions (i.e., same medium evolution, same choice of parton distribution functions, scale, etc.), all three jet energy-loss schemes yield very similar results. This finding is very encouraging, since it indicates that the technical aspects of the formalisms are well under control. However, we need to point out that there still exists a *puzzle* regarding the extracted

value for the transport coefficient $\hat{q}_0$, which spans a factor of 4 from a value of 2.3 GeV^2/fm for the HT approach on the lower end, to 4.1 GeV^2/fm for AMY and 10 GeV^2/fm for ASW on the high end, when using the same temperature scaling law for all three approaches. While the discrepancy among these approaches is not new, our work has been able to decisively rule out differences in the medium evolution or initial setup as a cause for the differing values of $\hat{q}$. We are led to conclude that these remaining differences are due to the different approximations applied, the different energy scales involved, and the different assumptions on the structure of the QCD matter inherent in these different approaches.

There exist multiple future directions for the systematic and unified approach to jet modification in dense matter presented here. Due to the assumption of a thermalized plasma, elastic energy loss may be straightforwardly included in AMY. Including elastic energy loss, however, represents a significant extension to the HT and ASW approaches, which has only recently been undertaken and thus this topic has not been included in the comparisons presented here. The current effort was restricted to single inclusive observables; hence, the simplest extension will be to apply a similar analysis to both single and multiparticle observables in tandem. Such comparisons will undoubtedly lead to stronger constraints on the formalism and hence deeper insights into the nature of the theory of jet modification used. Another direction is to use a somewhat different initial condition and equation of state for the medium evolution. A natural extension in this direction is to the study of jet modification in viscous fluid dynamical simulations. Viscous simulations necessarily seem to require an initial state with greater spatial anisotropy. We believe that it is in this direction that measurements and theoretical calculations of the R_{AA} vs the reaction plane will have most relevance, as a means to discriminate between different initial state profiles. The approximations that have resulted in the reduction of formalisms such as the HT and the ASW to a dependence on only one parameter will eventually have to be relaxed. The different parameters in these schemes represent actual physical properties of the produced matter which may indeed be measurable given a detailed and extensive set of experimental measurements.

ACKNOWLEDGMENTS

Authors C.G., G.Y.Q., and J.R. gladly acknowledge useful discussions with S. Caron-Huot, S. Jeon, and G. D. Moore. The authors also thank B. Müller for a careful reading of the manuscript. This work was supported in part by the US Department of Energy (Grant DE-FG02-05ER41367) (S.A.B., A.M., C.N.), the Academy of Finland, Project 206024 (T.R.), and the Natural Sciences and Engineering Research Council of Canada (C.G., G.Y.Q., J.R.).

[1] K. Adcox *et al.* (PHENIX Collaboration), Nucl. Phys. **A757**, 184 (2005).
[2] B. B. Back *et al.*, Nucl. Phys. **A757**, 28 (2005).
[3] J. Adams *et al.* (STAR Collaboration), Nucl. Phys. **A757**, 102 (2005).
[4] I. Arsene *et al.* (BRAHMS Collaboration), Nucl. Phys. **A757**, 1 (2005).
[5] M. Gyulassy and L. McLerran, Nucl. Phys. **A750**, 30 (2005).
[6] S. S. Adler *et al.* (PHENIX Collaboration), Phys. Rev. Lett. **91**, 172301 (2003).
[7] S. S. Adler *et al.* (PHENIX Collaboration), Phys. Rev. C **69**, 034909 (2004).
[8] J. Adams *et al.* (STAR Collaboration), Phys. Rev. Lett. **92**, 052302 (2004).
[9] K. Adcox *et al.* (PHENIX Collaboration), Phys. Rev. Lett. **88**, 022301 (2002).
[10] C. Adler *et al.* (STAR Collaboration), Phys. Rev. Lett. **89**, 202301 (2002).
[11] X.-N. Wang and M. Gyulassy, Phys. Rev. Lett. **68**, 1480 (1992).
[12] M. Gyulassy and X.-N. Wang, Nucl. Phys. **B420**, 583 (1994).
[13] X.-N. Wang, M. Gyulassy, and M. Plumer, Phys. Rev. D **51**, 3436 (1995).
[14] R. Baier, Y. L. Dokshitzer, A. H. Mueller, S. Peigne, and D. Schiff, Nucl. Phys. **B483**, 291 (1997).
[15] R. Baier, Y. L. Dokshitzer, A. H. Mueller, S. Peigne, and D. Schiff, Nucl. Phys. **B484**, 265 (1997).
[16] R. Baier, Y. L. Dokshitzer, A. J. Mueller, and D. Schiff, Phys. Rev. C **58**, 1706 (1998).
[17] B. G. Zakharov, JETP Lett. **63**, 952 (1996).
[18] B. G. Zakharov, JETP Lett. **65**, 615 (1997).
[19] B. G. Zakharov, Phys. Atom. Nucl. **61**, 838 (1998).
[20] M. Gyulassy, P. Levai, and I. Vitev, Phys. Lett. **B538**, 282 (2002).
[21] C. A. Salgado and U. A. Wiedemann, Phys. Rev. D **68**, 014008 (2003).
[22] S. Jeon and G. D. Moore, Phys. Rev. C **71**, 034901 (2005).
[23] X.-N. Wang, Phys. Lett. **B595**, 165 (2004).
[24] A. Majumder, Phys. Rev. C **75**, 021901(R) (2007).
[25] M. Gyulassy, I. Vitev, X.-N. Wang, and P. Huovinen, Phys. Lett. **B526**, 301 (2002).
[26] T. Renk and J. Ruppert, Phys. Rev. C **72**, 044901 (2005).
[27] T. Hirano and Y. Nara, Phys. Rev. C **66**, 041901(R) (2002).
[28] T. Hirano and Y. Nara, Phys. Rev. Lett. **91**, 082301 (2003), nucl-th/0301042.
[29] T. Hirano and Y. Nara, Phys. Rev. C **69**, 034908 (2004).
[30] C. Nonaka and S. A. Bass, Phys. Rev. C **75**, 014902 (2007), nucl-th/0607018.
[31] T. Renk, J. Ruppert, C. Nonaka, and S. A. Bass, Phys. Rev. C **75**, 031902(R) (2007).
[32] A. Majumder, C. Nonaka, and S. A. Bass, Phys. Rev. C **76**, 041902(R) (2007).
[33] G.-Y. Qin, J. Ruppert, S. Turbide, C. Gale, C. Nonaka, and S. A. Bass, Phys. Rev. C **76**, 064907 (2007).
[34] J. D. Bjorken, Phys. Rev. D **27**, 140 (1983).
[35] R. B. Clare and D. Strottman, Phys. Rep. **141**, 177 (1986).
[36] A. Dumitru and D. H. Rischke, Phys. Rev. C **59**, 354 (1999).
[37] P. F. Kolb, U. W. Heinz, P. Huovinen, K. J. Eskola, and K. Tuominen, Nucl. Phys. **A696**, 197 (2001).
[38] P. F. Kolb and U. W. Heinz, in *Quark-Gluon Plasma 3*, edited by R. C. Hwa and X.-N. Wang (World Scientific, Singapore, 2004).
[39] P. Huovinen, in *Quark-Gluon Plasma 3*, edited by R. C. Hwa and X.-N. Wang (World Scientific, Singapore, 2004).
[40] T. Hirano and K. Tsuda, Nucl. Phys. **A715**, 821 (2003).

[41] X.-F. Guo and X.-N. Wang, Phys. Rev. Lett. **85**, 3591 (2000).
[42] X.-N. Wang and X.-F. Guo, Nucl. Phys. **A696**, 788 (2001).
[43] B.-W. Zhang and X.-N. Wang, Nucl. Phys. **A720**, 429 (2003).
[44] A. Majumder, E. Wang, and X.-N. Wang, Phys. Rev. Lett. **99**, 152301 (2007).
[45] A. Majumder and B. Muller, Phys. Rev. C **77**, 054903 (2008).
[46] A. Majumder, R. J. Fries, and B. Muller, Phys. Rev. C **77**, 065209 (2008).
[47] U. A. Wiedemann, Nucl. Phys. **B582**, 409 (2000).
[48] U. A. Wiedemann, Nucl. Phys. **B588**, 303 (2000).
[49] C. A. Salgado and U. A. Wiedemann, Phys. Rev. Lett. **89**, 092303 (2002).
[50] N. Armesto, C. A. Salgado, and U. A. Wiedemann, Phys. Rev. Lett. **94**, 022002 (2005).
[51] P. Arnold, G. D. Moore, and L. G. Yaffe, J. High Energy Phys. 11 (2001) 057.
[52] P. Arnold, G. D. Moore, and L. G. Yaffe, J. High Energy Phys. 11 (2000) 001.
[53] S. Turbide, C. Gale, S. Jeon, and G. D. Moore, Phys. Rev. C **72**, 014906 (2005).
[54] M. Gyulassy, P. Levai, and I. Vitev, Nucl. Phys. **B571**, 197 (2000).
[55] M. Gyulassy, P. Levai, and I. Vitev, Nucl. Phys. **B594**, 371 (2001).
[56] M. Djordjevic and M. Gyulassy, Nucl. Phys. **A733**, 265 (2004).
[57] S. Wicks, W. Horowitz, M. Djordjevic, and M. Gyulassy, Nucl. Phys. **A784**, 426 (2007).
[58] J.-W. Qiu and G. Sterman, Nucl. Phys. **B353**, 105 (1991).
[59] A. Majumder, B. Muller, and S. A. Bass, Phys. Rev. Lett. **99**, 042301 (2007).
[60] A. Majumder and X.-N. Wang, Phys. Rev. D **70**, 014007 (2004).
[61] B. G. Zakharov, JETP Lett. **80**, 617 (2004).
[62] N. Armesto, C. A. Salgado, and U. A. Wiedemann, Phys. Rev. D **69**, 114003 (2004).
[63] U. A. Wiedemann, Nucl. Phys. **A690**, 731 (2001).
[64] E. Braaten and R. D. Pisarski, Phys. Rev. Lett. **64**, 1338 (1990).
[65] P. Arnold, G. D. Moore, and L. G. Yaffe, J. High Energy Phys. 06 (2002) 030.
[66] J. F. Gunion and G. Bertsch, Phys. Rev. D **25**, 746 (1982).
[67] G.-Y. Qin *et al*., Phys. Rev. Lett. **100**, 072301 (2008).
[68] E. Wang and X.-N. Wang, Phys. Rev. Lett. **87**, 142301 (2001).
[69] T. Renk and K. J. Eskola, Phys. Rev. C **75**, 054910 (2007).
[70] R. J. Fries, B. Muller, C. Nonaka, and S. A. Bass, Phys. Rev. Lett. **90**, 202303 (2003).
[71] M. Shimomura (PHENIX Collaboration), Nucl. Phys. **A774**, 457 (2006).
[72] R. Baier, Nucl. Phys. **A715**, 209 (2003).
[73] S. Caron-Huot and G. D. Moore (private communication).
[74] S. S. Adler *et al*. (PHENIX Collaboration), Phys. Rev. C **76**, 034904 (2007).
[75] R. J. Fries, B. Muller, C. Nonaka, and S. A. Bass, Phys. Rev. C **68**, 044902 (2003).
[76] A. Adare *et al*. (PHENIX Collaboration), Phys. Rev. C **77**, 064907 (2008).